

Crack Growth Model For Estimating The Fatigue Life Under Variable Loading

Hassan Abd- ALRsoul*, Basim H. Abbas*
& Khairallah S. Jabur*

Received on: 22/5/2011

Accepted on: 8/9/2011

Abstract

This paper examines the fatigue short and long cracks behaviour in 2024 T₄ aluminum alloy under rotating bending loading and stress ratio $R = -1$.

In the short cracks region, cracks grow initially at a fast rate but deceleration occurs quickly and, depending on the stress level, they either arrest or are temporarily halted at a critical length. This critical length is shown to coincide with the value of the microstructure parameter, grain size diameter,

An empirical model which describes short and long cracks rates is developed and is seen in good agreement with the experimental observations in this alloy. Comparison of the empirical model lives results with cumulative fatigue results has shown encouraging experimental agreement while Miner rule gave a non – reasonable prediction.

Keywords: Crack growth, Life prediction, Miner rule, Variable loading.

نموذج نمو الشق لتقييم اعمار الكلال تحت الاحمال المتغيرة

الخلاصة

يختبر هذا البحث تصرف شقوق الكلال الصغيرة والكبيرة لسبيكة الالمنيوم ذات الرمز 2024-T₄ تحت الحمل الانحنائي الدوراني وبنسبة اجهاد $R=-1$. منطقة الشقوق الصغيرة - نموها ابتدائياً بمعدل عالي وبعدها يحدث التباطؤ السريع وهذا يعتمد على مستوى الاجهاد. يأما هذه الشقوق تتوقف او تستقر مؤقتاً عند طول شق حرج. تم مشاهدة هذا الطول الحرج مطابقاً الى قيمة عامل التركيب المجهري وحجم الحبيبة. تم بناء انموذج رياضي معتمداً على النتائج العملية يصف نمو الشقوق الصغيرة والكبيرة، ولوحظ ان هذا الانموذج يتطابق بشكل جيد مع النتائج العملية، تم مقارنة اعمار الكلال المستخرجة عملياً من فحوصات تراكم الضرر مع الاعمار العملية واعطت هذه المقارنة توافق مشجع بينما نظرية ماينز اعطت تخمين غير معقول.

الكلمات المرشدة: نمو الشقوق، تخمين العمر، نظرية ماينز، التحميل المتغير.

Introduction

Static loads are rarely observed in modern engineering components or structures. By far, the majority of structures involve parts subjected to fluctuating or cyclic loads. For this reason, design analysts

must address themselves to the implications of Repeated loads, fluctuating loads, and rapidly applied loads. Such loading induces fluctuating or cyclic stresses

* Institute of Technology , Foundation of Technical Education /Baghdad

than often results in failure of the structure by fatigue. Indeed, it is often said that from 80% to 95% of all structural failures occur through a fatigue mechanism [1].

A fatigue failure can usually be recognized from the appearance of the fracture surface, which shows a smooth region, due to the rubbing action as the crack propagated through the section, and a rough region where the member has failed in a ductile manner when the cross-section was no longer able to carry the load.

The basic factors are necessary to cause fatigue failure, these are:

- Maximum tensile stress of sufficiently high value.
- Large enough variation or fluctuation in the applied stress.
- Sufficiently large number of cycles of the applied stress.

In addition, there are a host of other variables, such as stress concentration, corrosion, temperature, overload, metallurgical structure, residual stresses and combined stresses, which tend to alter the condition of fatigue [2].

The first aim of the present investigation is to study the behavior of short and long surface cracks via a surface replication technique. A second aim is to derive a model based on crack growth that can give accurate predictions of fatigue lifetime of plain specimen subjected to cumulative stress amplitude, variable loading, i.e. (low – high and high – low).

Experimental Details

2024-T₄ aluminum alloy used in this research had a wt% composition of 4.0 Cu: 0.244 Mg: 0.43 Mn: 0.43 Zn: 0.12 Si: 0.28 Fe: 0.1 Ni remainder

Al. Flat specimens were prepared from a raw material consisting of sheets of dimensions 500 x 500 mm. First, small rectangular sheets were cut to the dimensions of 34 x 92 mm. To get perfect dimensions of a fatigue specimen and to avoid mistakes, the desired profiles were machined to obtain the necessary holes. For this reason, four holes per specimen were done using fixed drill. The specimen is shown schematically in fig. (1).

Finishing Procedure

After machining, specimens were polished using the following steps:

- 1- Smoothing the specimen surface using different wet silicon carbide papers (200 to 1000 *m*m) for finishing.
- 2- Polishing the specimen using three different diamond lapping compounds (dialap).
 - Coarse compounds, average micron 3/2.
 - Fine compounds, average micron 1/1.
 - Extra – fine compound, average micron 0.25.

Distilled water was used for two minutes to clean the specimens followed by washing them with alcohol.

After washing operation, the surface roughness of the specimens was measured. The results are given in Table (1).

Tension test was executed to find out mechanical properties of material according to German engineering standard (DIN 50123).

The obtained values are shown in table (2)

The description of the machine and specimen calibration are given elsewhere [3].

The microstructure of the material (shown in fig. 2) consists of a fine grains of the diameters, which were measured using mean linear intercept method. This method gave the average grain size diameter of about 300 μm .

Experimental Results and Analysis of Crack growth observation

Replicas taken from some of the specimens tested at different values of stress amplitude and the replicas were subsequently observed, in the reverse order, in an optical microscope. The following information was thus obtained: number of cycles to the first sign of damage, number of cycles to the observation of cracks, crack length and crack growth rate. Full details of replication technique are given in reference [4].

The surface cracks and corresponding number of cycles are listed in table (3) for different stress levels.

The average crack length and crack speed (crack growth rate) are calculated from the data in table (3) and given in table (4).

The equations which best fit the present experimental data are [data of table (4)]

$$\frac{da}{dN} = AS^n (D - a_{av})^{n_1} \quad \text{For short cracks} \quad \text{----- (1)}$$

(Crack less than the average grain size diameter, D,)

With $A = 1.468 * 10^{-65}$, $n = 25.75$, $n_1 = 0.4173$ and

$$\frac{da}{dN} = BS^m a_{av}^{m_1} \quad \text{for long cracks} \quad \text{----- (2)}$$

(Cracks greater than the average grain size diameter, D,)

With $B = 3.972 * 10^{-15}$, $m = 4.292$ and $m_1 = 0.687$

The value of D in equation (1) which best fits the data is 300 μm , which is of the same order of the crack length threshold, i.e. $a_{th} = 300 \mu\text{m}$, calculated for this material [5]. This value of 300 μm is the same as the average grain size. More details of measuring and calculation of the average grain size can be found in reference [6].

Figure (3) shows the comparison of equation (1) and (2) with a set of experimental data.

Constant amplitude tests

Constant amplitude tests at different bending stresses, S_b , gave the results in table (3) and plotted in fig. (3)

Linear regression analysis was used to find the best relationship through the experimental points, i.e.

$$S_f = 1820 N_f^{-0.151} \quad \text{----- (3)}$$

The fatigue limit of $S_b = 159.6$ Mpa at 10^7 cycles with a confidence level of ± 3 Mpa

Cumulative fatigue damage results

In these tests a specimen is subjected to low – high and high – low fatigue loading. The results are tabulated in table (6).

Life Prediction methods and the crack growth equations

Of the numerous methods published to assess cumulative damage in fatigue, one of the most popular methods (Miner rule) will be applied to the results of the present experiments.

A new method is derived based on the short and long crack growth rate expressions, equation (1) and (2). This method is compared with the

palmgren Miner rule and the experimental fatigue lifetime results.

$$\sum \frac{n}{N_f} = \frac{n_1}{N_{f_1}} + \frac{n_2}{N_{f_2}} = 1 \quad \text{----- (4)}$$

This equation requires an expression for N_f as a function of stress (S) which can be obtained from constant amplitude tests, see equation (3)

Table (7) lists the values of the predicated life. The predication using the crack growth equations are very close to the experimental fatigue lives while palmgren – Miner gives non – conservative prediction.

Discussion

The Palmegren–Miner theory even through this theory has been proved erroneous on several occasions, it is still in common use because of its simplicity. When applying this rule to the low – high and high – low load pattern of the present test, it can be shown that. The main cause of error in palmgren – Miner prediction is that it consider damage to accumulate according to a parabolic law of defect growth at both high and low stresses. It is now known that this presumption is not true: Cracks less than a certain threshold length a_{th} or average grain size diameter (300 *mm*) propagates at an entirely different rate to cracks longer than a_{th} [7].

The method of prediction proposed here employ the two crack growth equation derived from experimental data obtained from constant amplitude tests. The short crack equation, equation (1), follows the model given by Miller etal [8] and Fatami and Yang [9] except that the plastic strain range is used to complement the long

crack law, equation (2), as proposed by Alalkawi [10].

In the present tests, therefore, the short crack region extends from a valve of $a = a_0$ (the initial roughness) to a value at which the short and long crack growth rates are identical: values of a_{th} or average grain size diameter. The long crack region extends from $a = a_{th}$ to $a_f = 19mm$, where a_f is the surface crack length at failure [11].

The short cracks behaviour can be related to the microscopic observations with the first stage corresponding to the growth of the crack along one set of slip bands.

Severe deceleration and arrest takes place when there is a sharp difference in the orientation of the adjacent grains.

Fig. (3) Shows that for short cracks the threshold for crack propagation is within the range 200 to approx. 400 *mm* . Above this limit LEFM (linear elastic fracture mechanics) analyses for long cracks may be applied. It follows that an equivalent crack be applied. It follows that an equivalent crack length value can be calculated by applying the concepts of LEFM to a crack at threshold conditions to a stress equal to the fatigue limit.

For the present case

$$\Delta K_{th} = Y \Delta S_0 \sqrt{p a_{th}} \quad \text{----- (5)}$$

Where ΔK_{th} is the threshold stress intensity factor range ΔS_0 is the bending fatigue limit stress and a_{th} is the threshold crack length. [4, 5, 6]

Conclusions

- 1- The initial crack growth rate of short cracks is high but they decelerate as they approach the

grain boundary , where , depending on the stress level they are either arrested or only temporarily halted,

- 2- The palmgren – Miner theory is not satisfactory for predicting life under low – high and high – low stress amplitude ,
- 3- Two distinct equations for fatigue crack growth rate, one for the short crack region and the other for long crack region, can be suitably combined to accurately predict the fatigue life of specimens tested under cumulative damage.

References

[1]Orkun Umer Onem, "Effect of Temperature on Fatigue Properties of DIN 35 NiCrMoV 12.5 steel", MSC thesis, Middle East technical university, 2003.

[2]Mahir Hameed Majeed, "Accumulated damage in Fatigue – Creep interaction of aluminum alloy 2024T₄ blade material", Phd thesis, University of Technology, 2009.

[3]Mohamed Faycal Ameer, "Shot peening effect in particular aircraft aluminum alloys", MSC thesis, University of Technology, 2002.

[4]De Los Rios, E. R. Mohamed Alalkawi H.J. and Miller, K.J. "A micromechanics analysis of short fatigue crack growth" fatigue fracture Enging . Mater, structures 8, 49 – 63, 1985.

[5]H. Hosseini – Toudesh and B. Mohmmedi "A simple method to

calculate the crack growth life of adhesively repaired aluminum panels", composite structure, 79, 234-241, 2007.

[6]Mohamed Al – alkawi H.J "cumulative fatigue damage under varying stress range conditions" PhD thesis university of sheffre ld" u.k., 1986.

[7]Anderikiv, O.E., Lesiv , R.M. and Levyts, N. M. "crack growth in structural materials under the combined action of fatigue and Creep" Materiald science, vol. 45, No.1, pp.7-24 , 2009 .

[8]Miller K. J. Mohamed Alalkawi H. J. and de los Rios, E. R. "Damage accumulation above and below the fatigue limit", the behaviour of fatigue short cracks EGF publ., Mechanical Engineering publication London. uk. pp. 491 – 511, 1986.

[9]Fatami, A. and Yang, L. "Cumulative fatigue damage and life prediction theories: a survey of the state of the art for homogeneous materials", Int. J. fatigue, vol. 20, No. 1, pp. 9-34, 1998.

[10]Al – alkawi H.J. "Fatigue damage Accumulation behaviour of 2024 Al – alloy under the effect of shot Peening time " Engineering and Technology Journal, university of Technology, 2008.

[11]Khairallah S. Jabur, “Surface Roughness Effect on Fatigue Life Perditions under Cumulative Damage” to be published, 2011.

Table (1): Surface roughness results of 9 specimens

Material	Average roughness Ra (m m)								
	A ₁	A ₂	A ₃	A ₄	A ₅	A ₆	A ₇	A ₈	A ₉
2024-T ₄	0.5	0.37	0.4	0.41	0.37	0.45	0.3	0.4	0.36

Table (2): Mechanical properties of material

S_u (Mpa)	S_y (Mpa)	Elongation %	HB	E (Gpa)	G (Gpa)
502	352	16	117	79	31

Table (3): crack length and number of cycles at three stress levels using replication technique

Specimen No. A ₁ Applied stress 300 Mpa	
(a) crack length (<i>m</i> m)	(N) No. of cycles (cycles)
120	10 ⁴
200	1.2 x 10 ⁴
350	1.5 x 10 ⁴
600	3 x 10 ⁴
1100	6 x 10 ⁴
2000	7 x 10 ⁴
2600	8 x 10 ⁴
3400	9 x 10 ⁴
4000	10 ⁵
Specimen No. A ₂ Applied stress 250 Mpa	
(a) crack length (<i>m</i> m)	(N) No. of cycles (cycles)
100	10 ⁴
180	3 x 10 ⁴
250	6 x 10 ⁴
450	7 x 10 ⁴
850	8 x 10 ⁴
1200	10 ⁵
1700	2 x 10 ⁵
2600	3 x 10 ⁵
3400	5 x 10 ⁵
4200	7 x 10 ⁵
Specimen No. A ₃ Applied stress 200 Mpa	
(a) crack length (<i>m</i> m)	(N) No. of cycles (cycles)
160	10 ⁵
250	2 x 10 ⁵
400	3 x 10 ⁵
800	4 x 10 ⁵
1200	5 x 10 ⁵
2000	6 x 10 ⁵
2600	8 x 10 ⁵
3000	10 ⁶

Table (4): Average crack length and crack growth rate results for different stress levels

Spec. No.	$a_{av} (mm)$ $(\frac{a_0 + a_1}{2})$	$\Delta a (mm)$ $(a_1 - a_0)$	ΔN (cycle) $(N_1 - N_0)$	$da/dN (mm/cycle)$ $(\Delta a / \Delta N)$
A ₁	60	120	10 ⁴	0.012
	160	80	0.2 x 10 ⁴	0.04
	275	150	0.3 x 10 ⁴	0.05
	475	250	1.5 x 10 ⁴	0.0166
	850	500	3 x 10 ⁴	0.0166
	1550	900	10 ⁴	0.09
	2300	600	10 ⁴	0.08
	3000	800	10 ⁴	0.08
3700	600	10 ⁴	0.06	

Spec. No.	$a_{av} (mm)$ $(\frac{a_0 - a_1}{2})$	$\Delta a (mm)$ $(a_1 - a_0)$	ΔN (cycle) $(N_1 - N_0)$	$da/dN (mm/cycle)$ $(\Delta a / \Delta N)$
A ₂	50	100	10 ⁴	0.01
	140	80	2 x 10 ⁴	4 x 10 ⁻³
	215	70	3 x 10 ⁴	2.3 x 10 ⁻³
	350	200	1 x 10 ⁴	0.02
	650	400	10 ⁴	0.04
	1025	350	2 x 10 ⁴	0.0175
	1450	500	10 ⁵	5 x 10 ⁻³
	2150	900	10 ⁵	9 x 10 ⁻³
	3000	800	2 x 10 ⁵	4 x 10 ⁻³
3800	800	2 x 10 ⁵	4 x 10 ⁻³	

Spec. No.	$a_{av} (mm)$ $(\frac{a_0 - a_1}{2})$	$\Delta a (mm)$ $(a_1 - a_0)$	ΔN (cycle) $(N_1 - N_0)$	$da/dN (mm/cycle)$ $(\Delta a / \Delta N)$
A ₃	80	160	10 ⁵	1.6 x 10 ⁻³
	205	90	10 ⁵	9 x 10 ⁻⁴
	325	150	10 ⁵	1.5 x 10 ⁻³
	600	400	10 ⁵	4 x 10 ⁻³
	1000	400	10 ⁵	4 x 10 ⁻³
	1600	800	10 ⁵	8 x 10 ⁻³
	2300	600	2 x 10 ⁵	3 x 10 ⁻³
	2800	400	2 x 10 ⁵	2 x 10 ⁻³

Table (5): S-N curve data at stress ratio R = -1

Spec. No.	S_f stress at failure (Mpa)	N_f (cycle) No. of cycles to failure
A ₄ , A ₅ , A ₆	400	40000 , 37000 , 33000
A ₇ , A ₈ , A ₉	300	8×10^4 , 9×10^4 , 10^5
A ₁₀ , A ₁₁ , A ₁₂	200	920 680 , 1.02×10^6 , 1.07×10^6

Table (6) cumulative fatigue tests results

Spec. No.	Applied stress levels (Mpa)	N_f (cycles)
B ₁	200 – 300	126460
B ₂	150 – 400	392562
B ₃	200 – 400	380500
B ₄	300 – 200	888640
B ₅	400 – 150	192650
B ₆	400 - 200	279650

Table (7) cumulative fatigue results, comparison case

Spec No.	N_f experimted	N_f from equations (1) and (2)	N_f Palmgren - Miner
B ₁	1126 460	709 769	286 944
B ₂	202 562	153 877	45 500
B ₃	300 550	298 706	45 120
B ₄	888 640	709 769	286 944
B ₅	192 650	153 877	45 500
B ₆	179 650	298 706	45 120

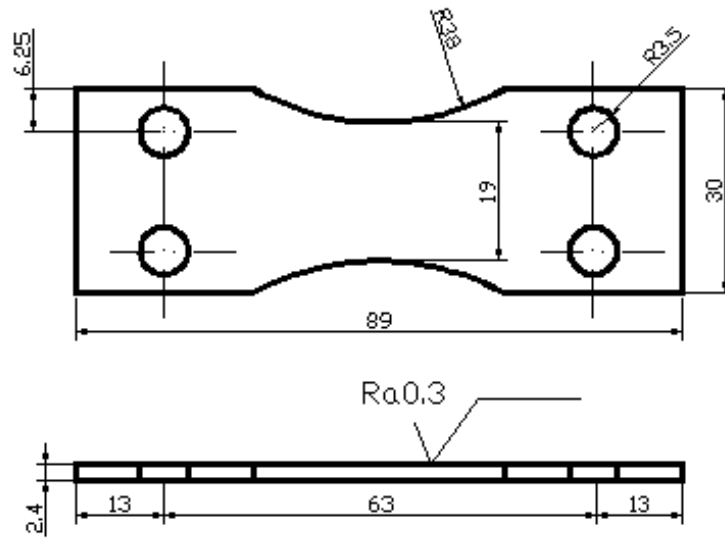


Figure (1): Reversed bending specimen geometry, dimensions in mm

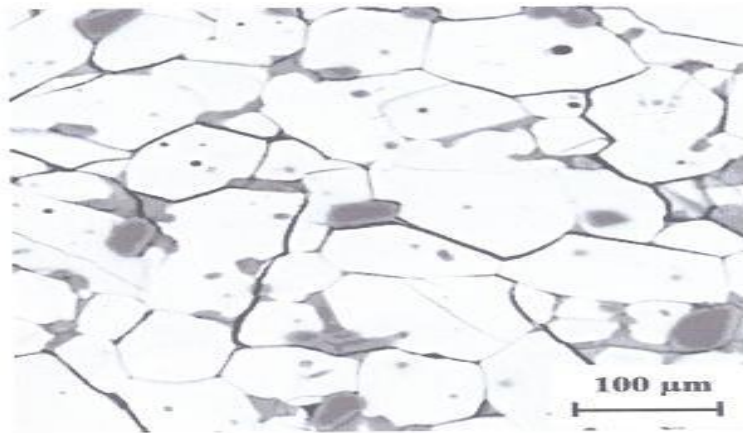


Figure (2) Microstructure of the material (2024-T4)

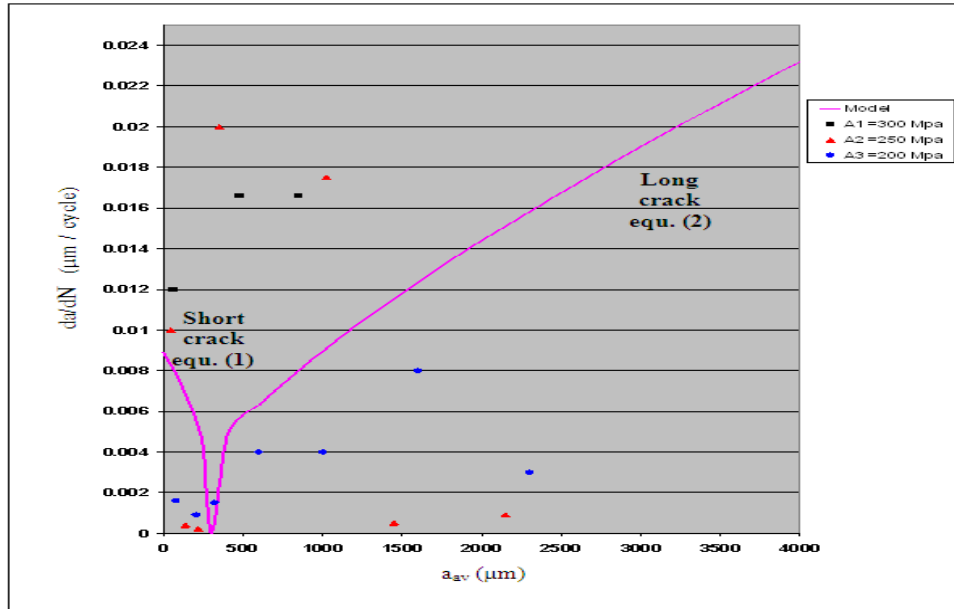


Figure (3) Experimentally determined surface crack growth rates at constant stress amplitude

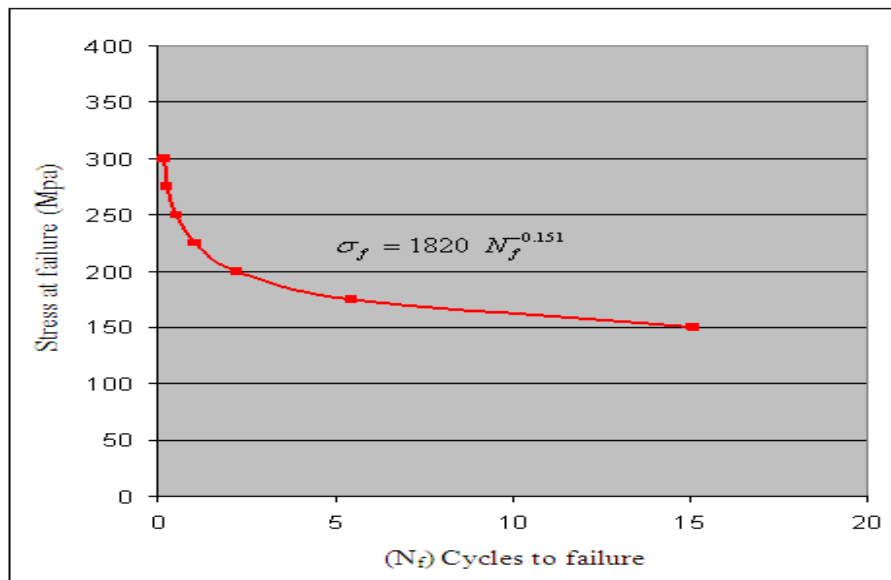


Figure (4) stress – No. of cycles fatigue life data